

Supplementary Information: Tailoring Metal-Dielectric Nanocomposite Materials with Ultrashort Laser Pulses for Dichroic Color Control

N. Sharma,^a N. Destouches,^{*a} C. Florian,^b R. Serna,^b J. Siegel^{*b}

^aUniv Lyon, UJM-Saint-Etienne, CNRS, Institut d'Optique Graduate School, Laboratoire Hubert Curien UMR 5516, F-42023 Saint-Etienne, France

^bLaser Processing Group, Instituto de Optica, Consejo Superior de Investigaciones Científicas (IO-CSIC), Serrano 121, 28006 Madrid, Spain

Fig. S1a) shows transmission, reflectance and loss spectra for the initial film. The 1-R-T values obtained show the existence of a weak absorption band for resonant laser excitation at the laser wavelength.

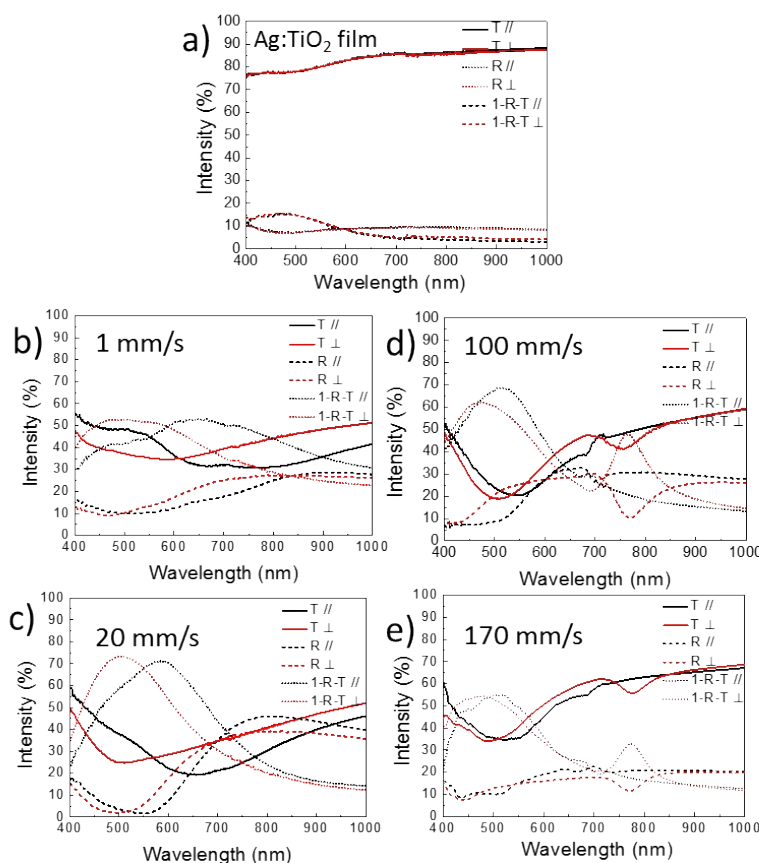


Figure S1 Spectral response of the nanostructures. Complementary data to the one shown in Fig. 6 of the main paper. The figures include transmission (T), reflectance (R) and loss (1-R-T) spectra. The losses spectra account for the absorption and scattering (calculated as (1-R-T)). ⊥ and // refers to the probe polarization, respective to the laser polarization. Spectra shown for a) the initial Ag:TiO₂ nanocomposite films before laser irradiation, and after irradiation at different scan speeds of b) 1 mm/s, c) 20 mm/s, d) 100 mm/s, and e) 170 mm/s.

Concerning the different types of nanostructures produced at different scan speeds (Fig. S1b-e)), the strong polarization anisotropy observed at low speeds in the transmission spectra is also confirmed in the loss spectra, markedly decreasing with scan speed. In parallel, the absorption bands increase in intensity upon an increase in speed and additional loss bands appear in the infrared region near 800 nm for speeds ≥ 100 mm/s. These bands correspond to the probe light that is coupled into the film acting as a waveguide, leading to a lower reflection and transmission and to a higher absorption. Coupling is mediated by the surface grating.

Fig. S2 displays the R, T and loss spectra of two representative nanocomposite films that were irradiated with a circular polarized laser beam, using scan speeds of 1 and 100 mm/s. The disappearance of anisotropy when using circular polarized light is confirmed also for the reflectance and loss spectra. The average of the experimental spectra for the two linear probe polarizations (Figure 6b and 6d) were calculated and displayed in Figure S2(c) and S2(d) for comparison. For $v = 1$ mm/s, the results are indeed equivalent, while for $v = 100$ mm/s, the resulting average curves are similar but show a significant deviation in the infrared region due to the existence of grating coupling and mode propagation for the structures fabricated with linear polarized laser light, and the absence of this behavior for circular laser light.

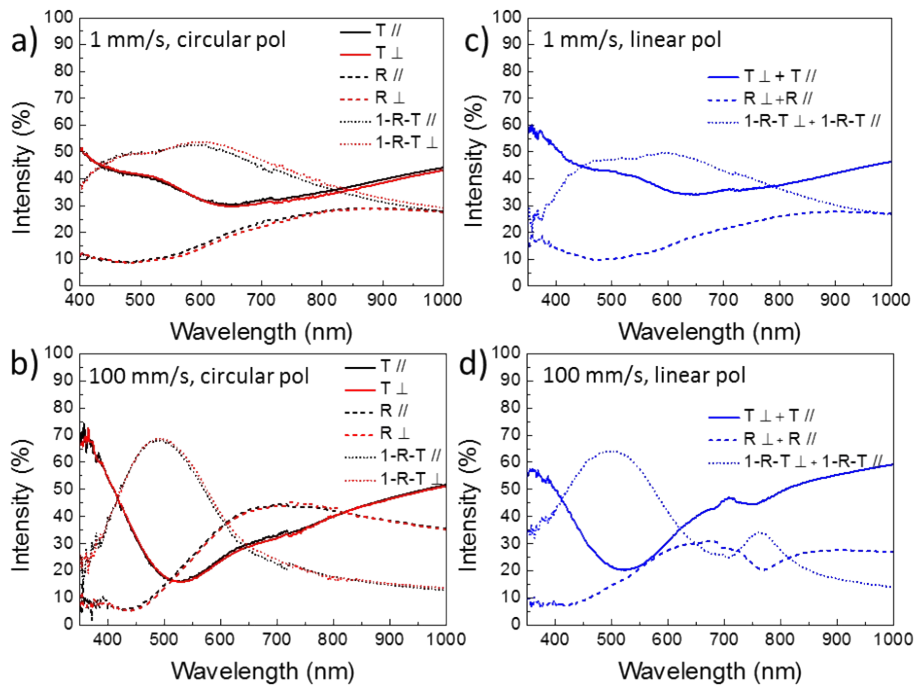


Figure S2: Elimination of spectral anisotropy by structuring with circular polarized laser light.

Complementary data to the one shown in Fig. 8 of the main paper. The figures include transmission (T), reflectance (R) and loss (1-R-T) spectra. The loss spectra account for the absorption and scattering (calculated as (1-R-T)). \perp and \parallel refers to the probe polarization, respective to the laser polarization. Spectra shown for nanostructures fabricated with circular polarized laser light for two different scan speeds. a) 1 mm/s and b) 100 mm/s. For comparison, c) and d) show curves for linear polarized laser light, obtained by calculating the average value of the experimental \perp and \parallel curves from Fig. 6b) and 6d). \perp and \parallel refers to the probe beam polarization, respective to the laser polarization.

The particle size distribution from the SEM images (Figure 2 of main text), for the four different speed regimes as described in the paper is shown below. It can be seen that for low speeds (1 mm/s, EG), the majority of nanoparticles grown are small, in the range of 10-20 nm, with a maximum size of up to 70 nm. When increasing the speed to 20 mm/s (no grating), the average nanoparticle size increases, ranging from around 15 nm to 80 nm in size, accompanied by a reduction in nanoparticle density. When the speed is increased further (100 mm/s, SG), the majority of nanoparticles grown are small, 10 nm in size with a maximum diameter of 50 nm. At the highest speed of 170 mm/s where the LIPSS with a higher height are obtained, again small nanoparticles are observed (10 nm), but these are accompanied by larger nanoparticles at the film surface, with a size up to 80 nm.

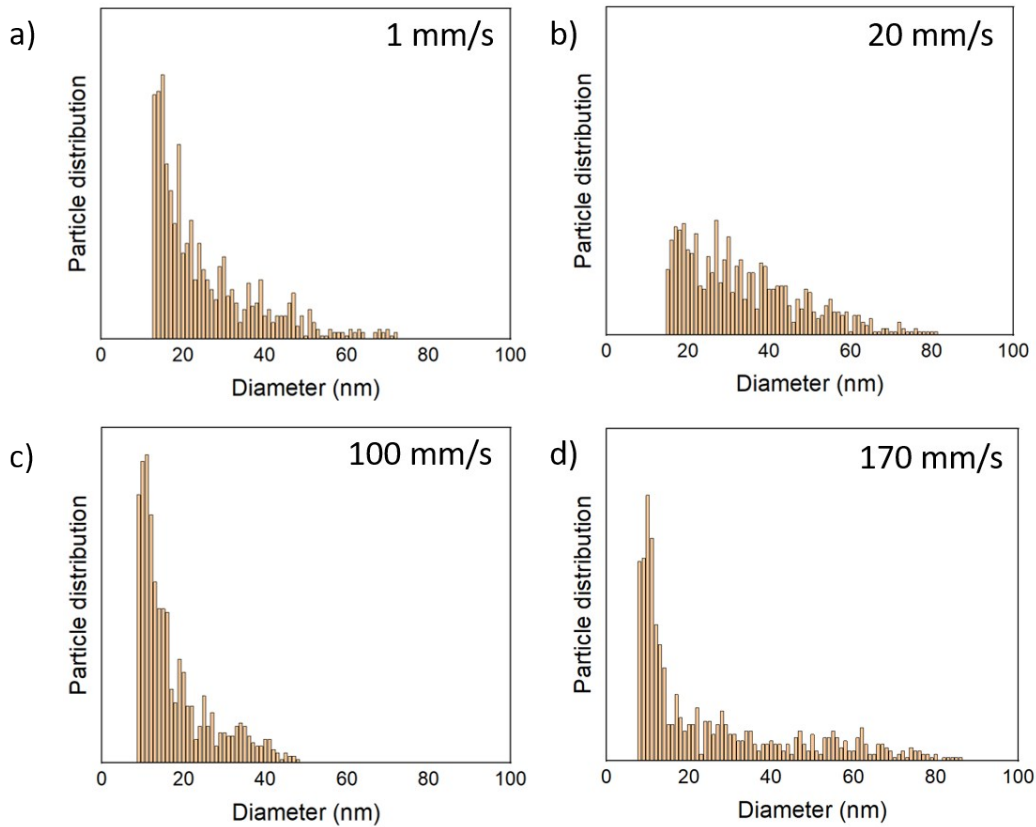


Figure S3: Size distributions of silver nanoparticles for different scan speeds. Size distributions, calculated from the SEM images (Figure 2 of paper) for four different scan speeds at a) 1 mm/s b) 20 mm/s c) 100 mm/s and d) 170 mm/s respectively.